LIMNOLOGY and OCEANOGRAPHY: METHODS

ASLO

Limnol. Oceanogr.: Methods 2023

doi: 10.1002/lom3.10584

A simple and low-cost open dynamic chamber for the versatile determination of methane emissions from aquatic surfaces

Víctor Germán Rodríguez-García,[1] Leobardo Ottmar Palma-Gallardo,[2] Francisco Silva-Olmedo,[1] Frederic Thalasso [1,3]*

[1]Department of Biotechnology and Bioengineering, Center for Research and Advanced Studies of the National Polytechnic Institute (Cinvestav), Mexico City, Mexico
[2]Department of Nanotechnology, Center for Research and Advanced Studies of the National Polytechnic Institute (Cinvestav), Mexico City, Mexico
[3]Cape Horn International Center for Global Change Studies and Biocultural Conservation (Chic), Universidad de Magallanes, Puerto Williams, Chile

Abstract

Methane (CH_4) emissions from aquatic ecosystems require accurate monitoring in the context of climate change. Among the several methods for CH_4 flux measurement, open dynamic chambers (ODC) are a reliable option. This method consists of a floating chamber through which a carrier gas is constantly flowing, providing accurate flux measurement with high temporal resolution. However, this method requires expensive and heavy CH_4 analyzers with high sensitivity, as well as a carrier gas system that comprises a gas cylinder and a gas flow controller, among other components. This system involves significant weight and cost challenges, limiting method implementation in certain settings and hindering its wider adoption. To address these limitations, we developed a simplified ODC configuration using atmospheric air as the carrier gas and a light and relatively less expensive detector. We applied this method to a 450-ha urban lake with CH_4 emissions ranging from moderate diffusive to high ebullitive fluxes. Concurrent measurements using a high-sensitivity CH_4 analyzer allowed us to compare the accuracy of the simplified ODC method and to assess its advantages and disadvantages. Results show that our method provides accurate CH_4 flux measurements with a spatial resolution comparable to high-sensitivity analyzers. This offers a more cost-effective, straightforward, and lightweight alternative to high-sensitivity detectors and carrier gas systems, simplifying ODC deployment in aquatic ecosystems.

Methane (CH_4) is a significant, long-lived greenhouse gas emitted in substantial quantities by aquatic ecosystems. Monitoring its emissions is crucial for establishing accurate greenhouse gas budgets in the context of climate change. It is estimated that $\sim 175.2 \pm 81.0$ Tg of CH_4 are emitted every year from lakes and reservoirs (Rosentreter et al. 2021). Additionally, other aquatic systems like wastewater infrastructures, treatment plants, stabilization ponds, constructed wetlands and others, are also important sources of atmospheric CH_4 (Saunois et al. 2020). In these natural and man-made systems, CH_4 emissions are largely variable, both temporally and spatially, within and among ecosystems, diel cycles, seasons, or regions of the world, varying over several orders of magnitude (Bastviken et al. 2011). The correct assessment of CH_4 emissions therefore requires significant field efforts as well as high-throughput methods to provide accurate and spatially representative data (D'Ambrosio and Harrison 2022).

Among the several reported methods for quantifying CH_4 emissions from aquatic surfaces, floating chamber methods are the predominant approach, used under numerous configurations. Chambers consist of an enclosure with an open bottom, floating on the water surface and capturing CH_4 emissions (Czepiel et al. 1993). In the standard application of the floating chamber, commonly referred to as closed dynamic chamber (CDC; Livingston and Hutchinson 1995), the CH_4 detector is connected to the chamber in a closed-circuit

*Correspondence: thalasso@cinvestav.mx

Author Contribution Statement: Conceptualization, V.G.R.G., F.T.; data acquisition, V.G.R.G., F.S.O., F.T.; data processing, V.G.R.G., L.O.P.G., F.T.; methodology, V.G.R.G., F.S.O., F.T.; project administration, F.T.; resources, F.S.O.; F.T.; writing–original draft, V.G.R.G., L.O.P.G., F.S.O., F.T.; writing–review & editing, V.G.R.G., F.T.

Additional Supporting Information may be found in the online version of this article.

configuration. This CDC configuration, also known as the non-steady-state method, is based on a CH_4 concentration build-up within the chamber, where flux can be determined from the increase rate. Chamber headspace is ventilated between measurements, either manually or through automatic venting systems (e.g., Duc et al. 2013; Martinsen et al. 2018). In a distinct configuration, named open dynamic chamber (ODC, Gerardo-Nieto et al. 2019), a well-defined carrier gas flows through the chamber, the CH_4 concentration is measured continuously at the outlet of the chamber, and CH_4 flux is determined from a mass balance equation. This method is also referred to as a steady-state method, since the system reaches equilibrium, it allows continuous measurements and does not require ventilation between measurements.

Whatever the method used, analyzers with high sensitivity (i.e., low limit of detection (LOD), standardly at sub-part-per-million, ppm) and high data acquisition frequency (standardly above 1 Hz) are often used because of their capability to quantify accurately low CH_4 emissions as well as to detect and interpret phenomena like ebullitive events (Villa et al. 2021) or non-linear concentration build-ups, often observed (Levy et al. 2011; Pihlatie et al. 2013; Silva et al. 2015). However, it is noteworthy that high sensitivity CH_4 analyzers (as listed on Supplementary Table S1) are often associated with elevated costs, significant weight (ranging from 5 to 15 kg), and substantial energy consumption (in the range of 20–50 W). These are obstacles that limit the spreading-out of high throughput chamber methods. To overcome these limitations, the use of low-cost semiconductor sensors has been suggested as a promising tool at an unrivaled low cost (Morawska et al. 2018; Bastviken et al. 2020). Despite the potential benefits of these semiconductor sensors for CH_4 flux measurements, their use is still limited by some drawbacks, including cross-sensitivity to non-target gases, the related need for calibration under the specific conditions of each ecosystem, and the requirement for self-made hardware/software assembling (Dey 2018; Bastviken et al. 2020). However, it is undeniable that these low-cost sensors hold the potential for significant improvement in CH_4 emissions studies in the future. In the meanwhile, the current market includes several models of ready-to-use medium-sensitivity detectors commercially available, which are significantly more cost-effective compared to high-sensitivity analyzers (Supplementary Table S1). These detectors could offer a more economical, straightforward, and lightweight alternative than high-sensitivity detectors while being widely available. Therefore, while we wait for semiconductor sensors to become more efficient and thoroughly applicable, medium-sensitivity analyzers could be a viable option for CH_4 flux measurements in aquatic ecosystems.

The spreading-out of high throughput ODC methods is also limited because they require a carrier gas, which implies heavy compressed gas cylinders and flow control systems onboard an accompanying boat. To simplify this requirement, the carrier gas could be replaced by fresh atmospheric air, flowing through the chamber, driven by a small pump. This modification would mean a much simpler and lighter chamber, promoting its deployment on aquatic ecosystems. Moreover, it is worth noting that most medium-sensitivity CH_4 detectors are equipped with an internal air pump, but do not have a point gas output, thus discarding their potential use in a closed circuit, as required in standard CDCs applications, but compatible with ODCs. Medium-sensitivity detectors therefore might fulfill both functions: measuring the CH_4 concentration and driving the carrier air flow through the chamber. This configuration would enable an easier assessment of CH_4 emissions in aquatic ecosystems, offering advantages such as cost-effectiveness and simplified deployment in remote locations while maintaining the high temporal resolution. Furthermore, since ODC methods involve a gas flowing through the chamber, their use limits the gas concentration build-up, observed in standard CDCs, in which the gas headspace is not renewed. Thus, the simplified ODC method suggested here might be compatible with medium- or long-term deployment without supervision.

Our aim in this study was to evaluate the feasibility of a simplified ODC configuration using (1) a commercially available and medium-sensitivity detector and (2) atmospheric air as a carrier gas. Specifically, we focused on assessing the accuracy of the proposed setup in quantifying CH_4 emissions from an aquatic ecosystem, analyzing its benefits and limitations. With these purposes, the simplified ODC setup was applied in a 450-ha urban lake, where CH_4 was previously identified to occur in a wide range from medium diffusive to high ebullitive flux. To assess the simplified ODC performance, the same measurements were done concomitantly with a high-sensitivity CH_4 analyzer. This strategy allowed the examination of methodological efficacy, as well as equipment performance in the measurement of diffusive and ebullitive CH_4 emissions under actual conditions, and comparing the results obtained with a well-validated detector.

Materials and procedures

Simplified ODC method

The simplified ODC method presented here shares some conceptual similarities with standard ODC methods and, for instance, with previous developments for the measurement of CH_4 macroseeps in lakes (Thalasso et al. 2020), or for the measurement of ebullitive fluxes in aquatic ecosystems (Gerardo-Nieto et al. 2019). However, the notable differences of the present method are: (1) the use of atmospheric air as a carrier gas instead of compressed gases, (2) the measurement of both diffusive and ebullitive emissions, in a wide range of magnitude, (3) the stationary deployment of the chamber during measurements, and (4) the use of a medium-sensitivity detector. Hence, the concept of the simplified ODC method is based on atmospheric air flowing constantly through a chamber that has an open bottom and that is floating on the water surface,

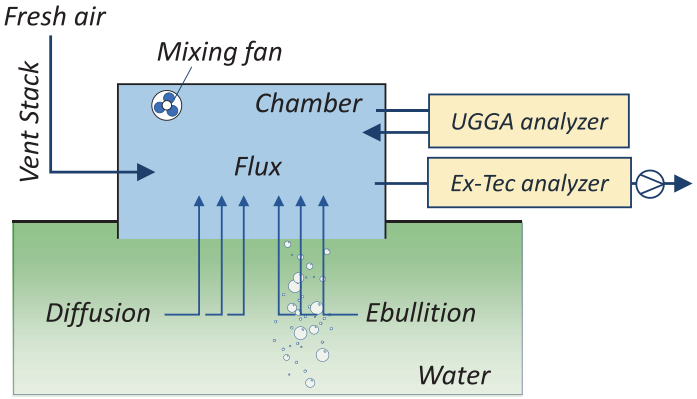

Fig. 1. Operation of the ODC: an open, inverted container (in blue) is positioned on the surface of a water body (in green). Methane emitted at the water surface is collected by the chamber and homogenized using a small fan. The air inside the chamber is extracted by the internal pump of a medium-sensitivity analyzer (Ex-Tec, see next section for details) and is replaced with fresh atmospheric air through the vent stack. A high-sensitivity detector analyzer (UGGA, see next section for details) operates in a closed loop, continuously sampling, analyzing, and discharging the measured air back into the chamber.

capturing CH_4 emissions that can be diffusive and/or ebullitive. The CH_4 emitted by the water surface and captured by the chamber is mixed with the carrier air, which is then measured by the detector, at the outlet of the chamber (Fig. 1).

A detailed description of this chamber mass balance is presented in the supplementary material Data S1. Briefly, the CH_4 mass balance between the chamber input and output gives:

$$F = \left(\frac{dC_m}{dt} + \frac{C_m \cdot Q_D}{V_C}\right) \times \frac{V_C}{A_C} = \left(\frac{dC_m}{dt} + \frac{C_m}{\theta}\right) \times \frac{V_C}{A_C} \quad (1)$$

where F (g m^{-2} s^{-1}) is the flux captured by the chamber, C_m (g m^{-3}) is the CH_4 concentration measured by the detector, Q_D is the air flowrate extracted by the analyzer, A_C (m^2) and V_C (m^3) are the area and the volume of the chamber, respectively, and θ (s) is the mean gas residence time within the chamber (V_C/Q_D).

Equation 1 shows that F can be continuously determined at any time during chamber deployment, providing measurements with enhanced time resolution. This approach has the potential to enable the detection of ebullitive events, although further demonstration is required. Moreover, it also mitigates the possible impact of concentration build-up, which has been observed with CDCs during medium- or long-term deployments (Xiao et al. 2016). These aspects will be further discussed in the Results and discussion section.

Experimental setup

For this work, a medium-sensitivity CH_4 detector was selected (Ex-Tec, HS 680, Sewerin, Germany), which is a relatively light (1 kg) and portable CH_4 analyzer equipped with an internal pump at a measured flowrate of 2.04 ± 0.05 L min^{-1}. This detector includes two CH_4 sensors: an infrared sensor and a gas-sensitive semiconductor, which together provide a measurement range of 1 ppm–100% vol. This detector includes a data-logger with a 1 Hz frequency. It is worth noting that the Ex-Tec detector requires field zeroing with atmospheric air. This was done regularly, in the field, by positioning the inlet of the Ex-Tec at the inlet of the vent stack. This strategy allowed for measurement of CH_4 concentration in excess to atmospheric air, simplifying the mass balance equations, as shown in the supplementary material Data S1. In complement to the Ex-Tec analyzer, an ultraportable greenhouse gas analyzer (UGGA, Los Gatos Research Inc, USA) was also used, for reference and comparison purposes. The Ex-Tec detector was connected to the chamber in an open-circuit configuration, thus measuring the CH_4 concentration within the chamber while ensuring the carrier air flow. On the contrary, the UGGA was connected in a closed loop from/to the chamber, measuring the same CH_4 concentration as the Ex-Tec, but with no effect on the gas flow passing through the chamber and therefore with no effect on the Ex-Tec measurements. Thus, both detectors were measuring CH_4 concentration under the same pneumatic regime, and the UGGA measurements were used as confirmative of those provided by the Ex-Tec.

The floating chamber previously described (Thalasso et al. 2020), was self-made from aluminum foils, has a volume of 7.5×10^{-3} m^3 and an open area in contact with water of 73×10^{-3} m^2. Inside the chamber, a small 2 in. battery-energized fan ensures gas mixing. Atmospheric air input is done through a vent stack made of 0.04 mm internal diameter polyurethane tubing, placed inside a 1.5 m aluminum tube. The chamber was operated from a small boat and, between measurements, the chamber was raised above water for 3 min, for ventilation purposes. In total, 64 flux measurements were done in Lago de Guadalupe, a Mexican polluted reservoir (see the Assessment section), over 6 min each.

Data treatment and statistical treatment

The Ex-Tec detector used in this study provides rounded values of C_m (measured concentration) and rounding depends on the magnitude of the measured value. Specifically, for concentrations in the range of 1–10 ppm, C_m is rounded to the nearest whole number in ppm units. For concentrations in the range of 10–100 ppm, C_m is rounded to the nearest two-unit ppm interval. For concentrations in the range of 100–1000 ppm, C_m is rounded to the nearest 20-unit ppm interval. For concentrations above 1000 ppm, C_m is registered with 200 ppm intervals. Because of this rounding, the C_m data exhibit step increases or decreases that do not accurately reflect the actual behavior of C_m. To address this issue, a polynomial smoothing technique was employed to mitigate the impact of rounding on the C_m data, using a Savitzky–Golay filter (Krishnan and Seelamantula 2013). From the smoothed C_m data obtained during chamber deployment, the instantaneous flux obtained with the Ex-Tec ($F_{Ex\text{-}Tec}$) was determined

according to Eq. 1. In parallel, data obtained with the UGGA were treated according to Gerardo-Nieto et al. (2019). The different data treatment approaches for the Ex-Tec and the UGGA are based on two reasons. First, unlike the Ex-Tec detector, the UGGA detector incorporates a cavity—a container through which the laser beam passes as it interacts with the sampled air. This design feature introduces a notable response time, caused by the mixing of the incoming sampled gas with the gas already contained in the cavity. Consequently, UGGA data treatment is slightly more extensive than Ex-Tec data treatment, in order to accurately calculate the real-time concentration of the gas entering the analyzer, as described in detail in Gerardo-Nieto et al. (2019). Secondly, unlike the Ex-Tec, the UGGA does not automatically adjust atmospheric concentration to zero, but measures the actual CH_4 concentration. Both the UGGA and the Ex-Tec provide results in volume fraction (ppm). The conversion to mass concentrations (mg m^{-3}) was done using the ideal gas law, considering the atmospheric pressure (0.77 atm) and temperature (20–23°C) during the measurement campaign.

According to Eq. 1, a key factor for data interpretation is the mean gas residence time within the chamber (θ), which depends on the flowrate extracted by the Ex-Tec (Q_D) and the volume of the chamber. The first option to determine θ is to measure the gas flowrate extracted by the Ex-Tec and calculating the volume of the chamber. Another option is to deploy the chamber in a section of the lake where diffusive fluxes are observed and to maintain the measurement until steady state is observed. According to Eq. 1, an asymptotic shape is then observable, that can be described by a logistic function of a continuous stirred tank reactor (Eq. 2), which can be easily calibrated using C_f and θ as adjustment parameters, minimizing the root mean square error with the solver function of Excel.

$$C_t = C_0 + (C_f - C_0) \times (1 - \exp(-t/\theta)) \tag{2}$$

where C_t is the measured concentration at a given time t, C_0 is the initial concentration, and C_f is the final concentration.

From the emissions data, we built contour maps by interpolation using Surfer 20.1.195 (Golden Software, USA). Surfer provides 10 interpolation methods, from which the best was chosen by evaluating the mean absolute error (MAE) and the mean bias error (MBE; Willmot and Matsuura 2006). From the interpolated flux matrices, we examined the flux spatial distribution, using a numerical homogeneity model (NHM; González-Valencia et al. 2019) on two datasets, each containing all Lago de Guadalupe fluxes obtained by Ex-Tec and UGGA. Briefly, the model establishes a homogeneity factor (h) that gives a numerical value to the spatial distribution of CH_4 fluxes over the entire lake, i.e., one h value for the entire ecosystem. For the determination of h, the interpolated emission data of Lago de Guadalupe were used as a set of areas ($A = A_1$, A_2, … A_i, … A_n), each associated with a flux ($F = F_1$, F_2, … F_i … F_n). Next, we multiplied the flux data F_i by the corresponding A_i to obtain a quantity of CH_4 emitted per unit of time ($M = M_1$, M_2, … M_i … M_n). The vector M was then reordered so that $M_1 \geq M_2 \geq \ldots \geq M_n$, keeping the corresponding A_i for each M_i. We finally established a cumulative normalized parameter M'_j (Eq. 3) ranging from 0 to 1, which is coupled to a cumulative normalized A' function (Eq. 4).

$$0 \leq M'_j = \frac{\sum_{i=1}^{j} M_i}{\sum_{1}^{n} M_i} \leq 1 \tag{3}$$

$$0 \leq A'_j = \frac{\sum_{i=1}^{j} A_i}{\sum_{1}^{n} A_i} \leq 1 \tag{4}$$

The spatial distribution of CH_4 fluxes in the ecosystem was then obtained by plotting the pair (M'_j, A'_j), and homogeneity was described by h (%; Eq. 5). The significance of this quantity is that for a homogeneous distribution, $h = 100\%$, while for a nonhomogeneous distribution, $0 \leq h < 100\%$.

$$0 \leq h = \frac{1 - \int_0^1 M' dA'}{0.5} \cdot 100 \leq 100\% \tag{5}$$

In addition, a second parameter, denoted as $A^{\%}$, was introduced to quantify the proportion of the entire ecosystem area that contributes a specific percentage of the overall emission. The superscript % corresponds to the designated percentage, ranging from 0% to 100% of the total emission. For instance, A^{80} represents the percentage of the ecosystem area responsible for 80% of the total emission. Importantly, it should be noted that if a particular section of the ecosystem does not emit CH_4, the corresponding A^{100} value will be < 100%.

Assessment

The method was tested in Lago de Guadalupe on November 2nd, 3rd, and 8th, 2022, during the day, from ~ 10:00 h until 16:00 h. Lago de Guadalupe is located within Mexico City metropolitan area at 2240 m a.s.l. and 25 km northwest of the center of Mexico City (lat. 19.6325, long. −99.2555), Lago de Guadalupe is a eutrophic 450-ha urban reservoir previously characterized (Sepúlveda-Jauregui et al. 2013; Aguirrezabala-Cámpano, et al. 2021). The lake has a maximum depth of 19 m, and three polluted rivers carry urban rain/wastewater discharges into the reservoir, at its western section (Sepúlveda-Jauregui et al. 2013).

The simplified ODC method was implemented at 64 strategically chosen sites spanning across the diverse regions of

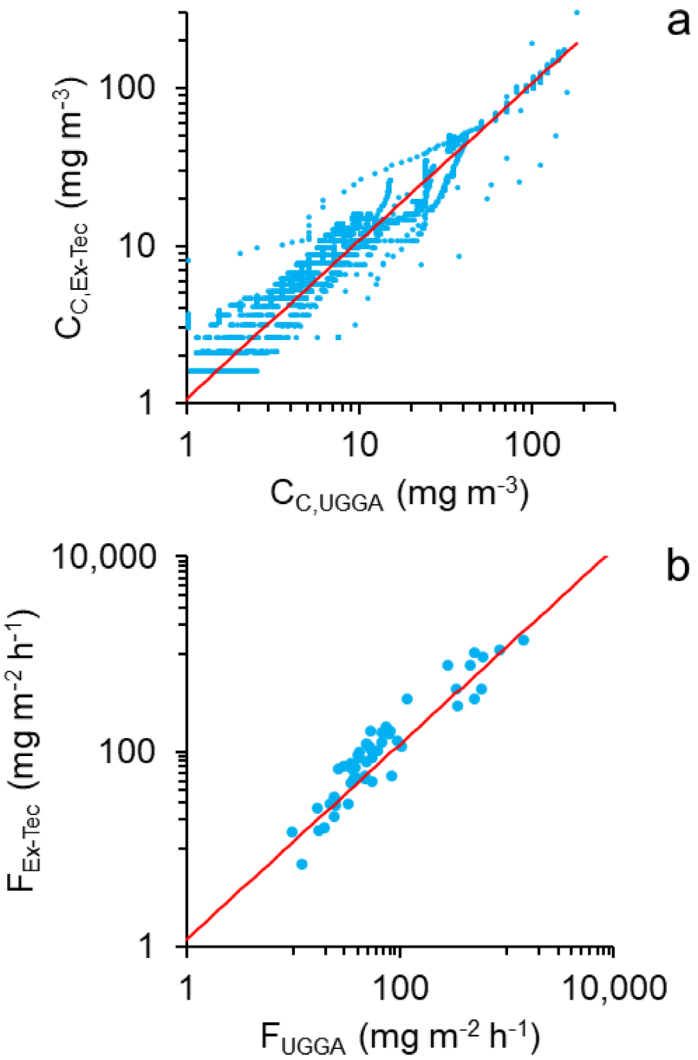

Fig. 2. Correlation between CH_4 concentrations (**a**) and fluxes (**b**) measured with the UGGA and Ex-Tec analyzers.

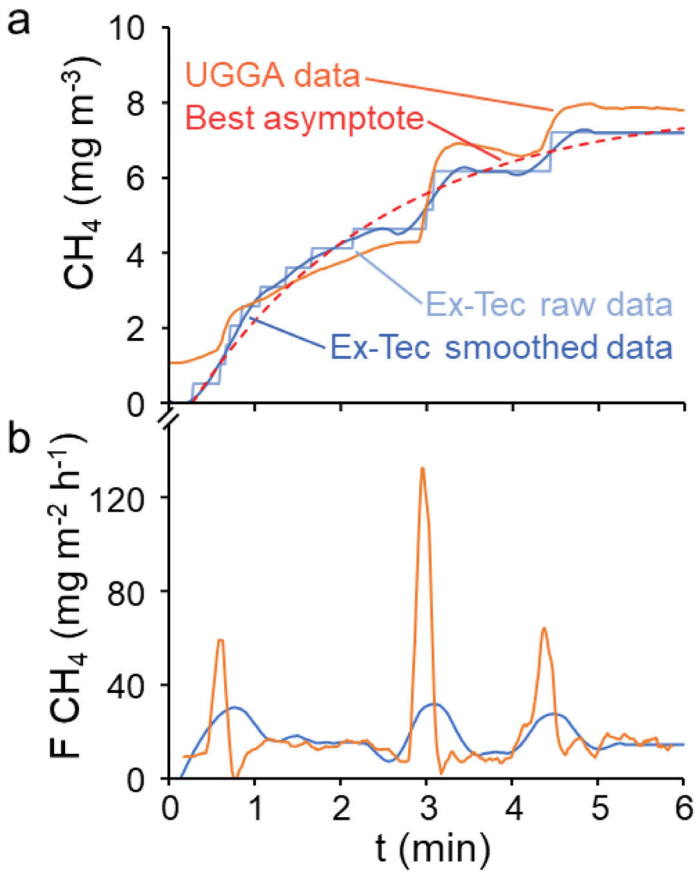

Fig. 3. Example of ODC chamber deployment; (**a**) CH_4 concentration measured with the Ex-Tec (blue lines) and the UGGA (orange continuous line) and the best asymptotic model calibration based on Ex-Tec data; (**b**) instantaneous flux determined with both detectors (same colors as panel a).

Lago de Guadalupe, including the littoral and limnetic zones, as well as areas with prominent wastewater discharges and more preserved areas. Hence, the sampling strategy covered the widest possible range of CH_4 emissions, from medium diffusive to high ebullitive fluxes. During flux measurement, both the Ex-Tec and the UGGA detectors recorded similar CH_4 concentrations (Fig. 2a). Overall, the coefficient of determination (r^2) between both measurements was 0.971 and the slope of the correlation was 1.045 ($p < 0.001$), suggesting that Ex-Tec overestimated by 4.5% the CH_4 concentration. The main factor that might explain the differences between both methods is the value rounding by the Ex-Tec detector, which is observable in Fig. 2a with clusters of horizontally dispersed data points. In this regard, to evaluate the impact of Ex-Tec data smoothing using the Savitzky–Golay filter, we compared UGGA CH_4 concentrations with Ex-Tec smoothed data (Supporting Information Fig. S2). The results showed a similar correlation (slope 1.08; $r^2 = 0.950$; $p < 0.001$), indicating that data smoothing had no significant impact on the mean concentration readings.

An example of CH_4 concentrations observed during flux measurement is depicted in Fig. 3a, and three additional examples are provided in Supporting Information Fig. S3 for reference, covering a wide range of CH_4 fluxes. As anticipated, in accordance with the expected behavior of the ODC, the CH_4 concentration exhibited an asymptotic increase toward steady-state values, with noticeable irregularities, likely attributable to emissions variability and ebullitive events. Nonetheless, the overall trend of the asymptotic curves aligned well with the anticipated behavior, with a θ value of 180.3 ± 4.5 s, experimentally determined. This confirms the appropriateness of the continuous stirred tank reactor model in describing the pneumatic behavior of the ODC chamber. Notably, Fig. 3a (as well as Supporting Information Fig. S3) shows that the UGGA provided continuous unrounded data, while the Ex-Tec data exhibited clear step increases due to rounding and range switching, which were successfully smoothed with the Savitzky–Golay filter.

After applying Eq. 1, Fig. 3b (and Supporting Information Fig. S3) shows the instantaneous flux determined with the Ex-Tec ($F_{Ex\text{-}Tec}$, Eq. 1), and the UGGA. Notably, F_{UGGA} indicates clear ebullitive events, noticeable by peaks in the instantaneous flux curve. These peaks allow to segregate diffusive and ebullitive flux data as previously described in Gerardo-Nieto et al. (2019). Briefly, the data interpretation consists in segregating peaks in the F_{UGGA} graph, to calculate the mean diffusive flux from the remaining data. Then, the total flux is determined from the average of all measurements, and ebullitive flux is determined from the difference between total and diffusive flux. In the case of $F_{Ex\text{-}Tec}$ also presented in Fig. 3b, the peaks appear significantly smoothed, due to the automatic rounding by the Ex-Tec detector and the subsequently applied Savitzky–Golay filter. Hence, in many cases, the data provided by the Ex-Tec prevented a clear identification of ebullitive events, although the determination of the total flux was not affected.

Flux measurements obtained using Ex-Tec and UGGA detectors (see Table 1, Fig. 2b) displayed a strong positive correlation ($r^2 = 0.889$; $p < 0.001$). However, it is worth noting that there was a slight discrepancy in the slopes, with Ex-Tec measurements generally showing a 19% overestimation when compared to those obtained using the UGGA analyzer. Furthermore, as it will be shown in the next subsection, from interpolated data, the total emission estimated with Ex-Tec data, was 8.4% higher than the total emission determined with UGGA data. In the absence of a third validated and exact method for comparison, we cannot conclusively determine which equipment provides the most accurate results. Overall, fluxes varied over almost three magnitude orders and ranged from a few mg to several g m^{-2} h^{-1}, significantly higher than fluxes reported in the literature for lakes, reservoirs and wetlands ($p < 0.05$; Supporting Information Fig. S4). The latter confirms the polluted/eutrophicated nature of Lago de Guadalupe previously reported (Sepúlveda-Jauregui et al. 2013; González-Valencia et al. 2014; Aguirrezabala-Cámpano et al. 2021).

Table 1. Statistical parameters of flux measurements and results of the ANOVA comparing Ex-Tec and UGGA detectors: *n*, number of independent chamber deployments; *m*, total instantaneous fluxes measurements; CV, coefficient of variation.

Parameter	Ex-Tec	UGGA	Note/units
n	64	64	
m	19,200	19,200	
Min	7.02	9.72	mg m^{-2} h^{-1}
Max	2001	2593	mg m^{-2} h^{-1}
Mean	287.67	235.73	mg m^{-2} h^{-1}
Stdev	410.13	497.96	mg m^{-2} h^{-1}
CV	143	211	%
F (ANOVA)	0.408		
F-crit (ANOVA)	3.916		

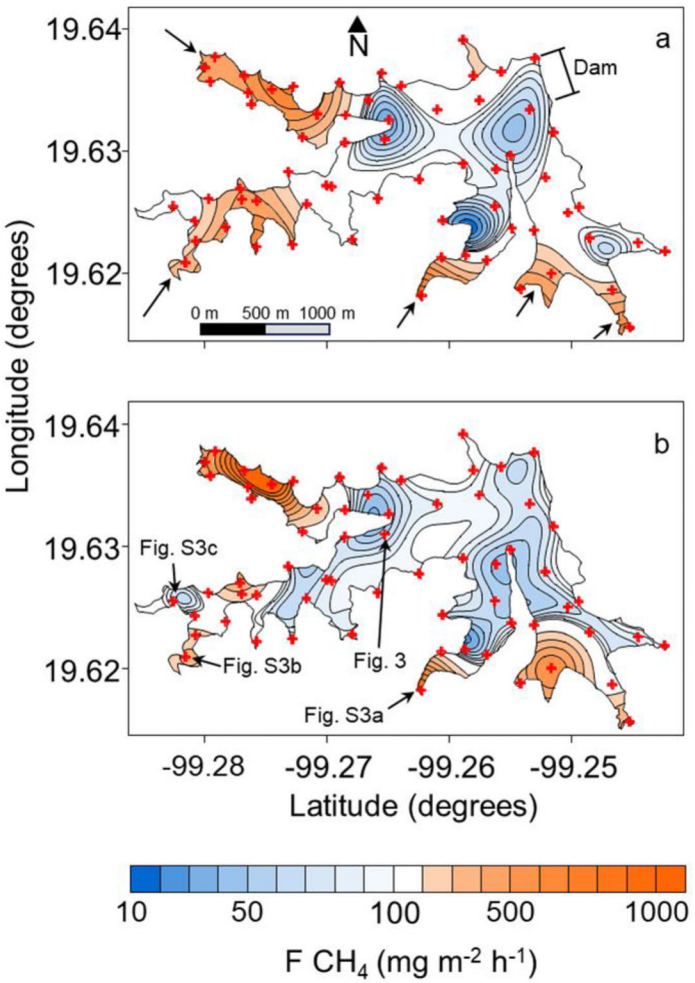

Fig. 4. Interpolated maps of CH_4 emissions in Lago de Guadalupe, as determined from the Ex-Tec detector (**a**) and the UGGA detector (**b**). Color intensity is related to flux values: Blue areas indicate lower CH_4 flux, orange areas indicate higher CH_4 flux. Red crosses indicate sampling sites. In Panel (a), arrows indicate wastewater discharges, and the location of the flux measurement examples (Fig. 3 and Supporting Information Fig. S3) are indicated in Panel (b).

From flux measurements with both detectors, interpolated contour maps were constructed (Fig. 4). The best interpolation method, among the 10 interpolation methods available in the Surfer Software, was Kriging, which minimized the MAE and the MBE (the fourth-lowest MAE and the MBE closest to zero). Supplementary Table S2 presents the results obtained using the 10 interpolation methods available in Surfer Software for Ex-Tec flux measurements, along with several statistical parameters. In both maps, generated through Kriging interpolation, we observed higher emissions in the western and southern arms of the lake, coinciding with the areas where most wastewater discharges occurred. Conversely, lower

emissions were detected near the dam and in the central section of the lake. Overall, two arguments suggest that medium-sensitivity detectors offer a similar spatial resolution in CH_4 emission studies than high-sensitivity detectors. First, the total CH_4 emission of the lake, determined from the interpolated matrices, was 45.0 and 41.5 kg h^{-1} from the Ex-Tec and the UGGA data, respectively. Second, when applying the NHM (Supporting Information Fig. S5), h was 60.0% for the $F_{Ex\text{-}Tec}$ map and 55.3% for the F_{UGGA} map. Similarly, in both maps, CH_4 emissions were always detected, and consequently A^{100} was 100% in both cases, i.e., no dead area. Regarding the area percentage responsible for 50% of the total emission, A^{50} was 21% for the Ex-Tec map and 16% for the UGGA map.

Discussion

The simplified ODC method, with a medium-sensitivity detector and the use of atmospheric air, allowed to quantify CH_4 total emissions, although without distinction between diffusive and ebullitive emissions, in a range of 7–2000 mg m^{-2} h^{-1}. A comparison between the simplified ODC method and standard CDCs, as well as the previously tested ODC (Gerardo-Nieto et al. 2019), reveals distinct advantages and drawbacks, as summarized in Supplementary Table S3. Furthermore, we find relevant discussing two specific key characteristics of the simplified ODC method; the LOD and the impact of concentration build up over flux measurement.

Given that the Ex-Tec has a LOD of 1 ppm (above atmospheric concentration), the theoretical minimum flux (F_{min}) that can be potentially measured by the simplified ODC method under steady state (Eq. 1) is 1.46 mg m^{-2} h^{-1} at 20°C and 1 atm. To determine in which fraction of aquatic ecosystems the simplified ODC method is likely to perform well, i.e., emissions above the LOD, we compiled flux data from Bastviken et al. (2011), Ortiz-Llorente and Álvarez-Cobelas (2012), and Deemer et al. (2016), encompassing datasets from 261 lakes, 72 reservoirs, and 318 wetlands (Supporting Information Fig. S4). From this analysis, we anticipate that our method would perform well in 51%, 39%, and 70% of the lakes, reservoirs, and wetlands, respectively, or 59% of all reported aquatic ecosystems. Thus, the method, under its current configuration, is limited to ecosystems with relatively large emissions, such as mesotrophic or eutrophic water bodies, and man-made systems such as wastewater infrastructures. However, the LOD of the method is not an absolute barrier, and Eq. 1 shows that large V_C, low Q_D, which together promote large θ, as well as a large A_C, would decrease the LOD of the method and increase the fraction of the ecosystems where the simplified ODC method could be successfully applied. To this regard, it should be mentioned that the ODC method presented here does not exclude a standard operation under CDC configuration, which can be achieved by closing the input of fresh atmospheric air and operating a detector with a point gas output, in a closed loop (not allowed with the Ex-Tec tested here). Thus, a further advantageous development of the ODC chamber would be to use a detector allowing facultative ODC/CDC operation, to allow flux measurement whatever the level of CH_4 emission.

Another aspect that is worth discussing is the impact of concentration build-up that potentially reduces the gas partial pressure gradient between the water surface and the atmosphere, altering CH_4 flux measurement. This important aspect has been well studied (Xiao et al. 2016; Mannich et al. 2019), and it has been suggested that open chambers are advantageous to this regard (Mu et al. 2022). Indeed, in standard CDCs, no steady state is reached, in such manner that the CH_4 concentration within the chamber (C_{CDC}) depends on flux and measurement duration (Eq. 6), while in ODCs, the CH_4 concentration within the chamber (C_{ODC}) reaches a steady-state (Eq. 7):

$$C_{CDC} = F \times \frac{A_C}{V_C} \times t \quad (6)$$

$$C_{ODC} = F \times \frac{A_C}{V_C} \times \theta \quad (7)$$

Thus, both CDC and ODC reach the same CH_4 concentration at a time $t = \theta$, and for any $t > \theta$, C_{CDC} surpasses C_{ODC}. Notably, θ is relatively short (e.g., 3 min in the present work) which is shorter than the standard deployment time of CDCs. Thus, if applied in the same conditions, C_{CDC} will typically exceed C_{ODC}, fostering the effects of CH_4 concentration build-up. A corollary of the latter is that ODC could be easily operated for extended periods, unsupervised, since C_{ODC} would never exceed the magnitude anticipated by Eq. 7. Moreover, unsupervised long-term operation of the ODC method would be simplified as it does not require mechanical devices to ventilate chamber headspace, such as those suggested by Duc et al. (2013) and Martinsen et al. (2018) for CDCs.

Comments and recommendations

While the simplified ODC method offers several benefits, CDCs still have some advantages, particularly in situations where low fluxes are observed. In such cases, CDC can be operated for long periods of time, until detectable C_{CDC} levels are reached. Therefore, a hybrid chamber design that allows for both ODC and CDC operation could be advantageous, especially when dealing with varying flux levels. In conclusion, the simplified ODC method presented in this study offers a cost-effective, lightweight, and easy-to-use alternative for measuring CH_4 fluxes in aquatic ecosystems, especially in remote areas. Our results show that the method is comparable to others, with more expensive and high-sensitivity detectors, in determining the spatial distribution of CH_4 emissions. Additionally, the simplified ODC allows for long-term deployments without supervision, improving temporal resolution. However, it should be noted that the method cannot

differentiate between diffusive and ebullitive emissions, although it provides total emissions data. Also, the simplified ODC method has a relatively high LOD, which may limit its application in ecosystems with low CH_4 emissions. Furthermore, we see the simplified ODC method as a technical basis for the integration of low-cost detectors as technology advances, allowing for more constrained and spatially resolved CH_4 flux measurements in aquatic ecosystems.

Data Availability Statement

The datasets generated during the current study are available from the corresponding author on reasonable request.

References

Aguirrezabala-Cámpano, T., R. González-Valencia, F. J. Cervantes, and F. Thalasso. 2021. Overall spatiotemporal dynamics of greenhouse gases and oxygen in two subtropical reservoirs with contrasting trophic states. Water Res. **196**: 117056. doi:10.1016/j.watres.2021.117056

Bastviken, D., L. J. Tranvik, J. A. Downing, P. M. Crill, and A. Enrich-Prast. 2011. Freshwater methane emissions offset the continental carbon sink. Science **331**: 50. doi:10.1126/science.1196808

Bastviken, D., J. Nygren, J. Schenk, R. Parellada Massana, and N. T. Duc. 2020. Technical note: Facilitating the use of low-cost methane (CH4) sensors in flux chambers–Calibration, data processing, and an open-source make-it-yourself logger. Biogeosciences **17**: 3659–3667. doi:10.5194/bg-17-3659-2020

Czepiel, P. M., P. M. Crill, and R. C. Harriss. 1993. Methane emissions from municipal wastewater treatment processes. Environ. Sci. Technol. **27**: 2472–2477. doi:10.1021/es00048a025

D'Ambrosio, S. L., and J. A. Harrison. 2022. Measuring CH4 fluxes from lake and reservoir sediments: Methodologies and needs. Front. Environ. Sci. **10**: 850070. doi:10.3389/fenvs.2022.850070

Deemer, B. R., and others. 2016. Greenhouse gas emissions from reservoir water surfaces: A new global synthesis. Bioscience **66**: 949–964. doi:10.1093/biosci/biw117

Dey, A. 2018. Semiconductor metal oxide gas sensors: A review. Mater. Sci. Eng. **229**: 206–217. doi:10.1016/j.mseb.2017.12.036

Duc, N. T., S. Silverstein, L. Lundmark, H. Reyier, P. Crill, and D. Bastviken. 2013. Automated flux chamber for investigating gas flux at water–air interfaces. Environ. Sci. Technol. **47**: 968–975. doi:10.1021/es303848x

Gerardo-Nieto, O., A. Vega-Peñaranda, R. González-Valencia, Y. Alfano-Ojeda, and F. Thalasso. 2019. Continuous measurement of diffusive and ebullitive fluxes of methane in aquatic ecosystems by an open dynamic chamber method. Environ. Sci. Technol. **53**: 5159–5167. doi:10.1021/acs.est.9b00425

González-Valencia, R., A. Sepúlveda-Jauregui, K. Martínez-Cruz, J. Hoyos-Santillán, L. Dendooven, and F. Thalasso. 2014. Methane emissions from Mexican freshwater bodies: Correlations with water pollution. Hydrobiologia **721**: 9–22. doi:10.1007/s10750-013-1632-4

González-Valencia, R., F. Magaña-Rodríguez, A. Sepúlveda-Jauregui, T. Aguirrezabala-Cámpano, O. Gerardo-Nieto, and F. Thalasso. 2019. A simple model for the numerical characterization of spatiotemporal variability in aquatic ecosystems. Aquat. Sci. **81**: 58. doi:10.1007/s00027-019-0652-1

Krishnan, S. R., and C. S. Seelamantula. 2013. On the selection of optimum Savitzky-Golay filters. IEEE Trans. Signal Process. **61**: 380–391. doi:10.1109/TSP.2012.2225055

Levy, P. E., and others. 2011. Quantification of uncertainty in trace gas fluxes measured by the static chamber method. Eur. J. Soil Sci. **62**: 811–821. doi:10.1111/j.1365-2389.2011.01403.x

Livingston, G. P., and G. L. Hutchinson. 1995. Enclosure-based measurement of trace gas exchange: Applications and sources of error, p. 14–51. *In* R. C. Harriss and P. A. Matson [eds.], Biogenic trace gases: Measuring emissions from soil and water. Blackwell Science Ltd.

Mannich, M., C. V. S. Fernandes, and T. B. Bleninger. 2019. Uncertainty analysis of gas flux measurements at air-water interface using floating chambers. Ecohydrol. Hydrobiol. **19**: 475–486. doi:10.1016/j.ecohyd.2017.09.002

Martinsen, K. T., T. Kragh, and K. Sand-Jensen. 2018. A simple and cost-efficient automated floating chamber for continuous measurements of carbon dioxide gas flux on lakes. Biogeosciences **15**: 5565–5573. doi:10.5194/bg-15-5565-2018

Morawska, L., and others. 2018. Applications of low-cost sensing technologies for air quality monitoring and exposure assessment: How far have they gone? Environ. Int. **116**: 286–299. doi:10.1016/j.envint.2018.04.018

Mu, J., J. Qi, H. Yu, C. Hu, Y. Mu, and J. Qu. 2022. Dynamic chamber as a more reliable technique for measuring methane emissions from aquatic ecosystems. Sci. Total Environ. **851**: 158147. doi:10.1016/j.scitotenv.2022.158147

Ortiz-Llorente, M. J., and M. Álvarez-Cobelas. 2012. Comparison of biogenic methane emissions from unmanaged estuaries, lakes, oceans, rivers and wetlands. Atmos. Environ. **59**: 328–337. doi:10.1016/j.atmosenv.2012.05.031

Pihlatie, M. K., and others. 2013. Comparison of static chambers to measure CH4 emissions from soils. Agric. For. Meteorol. **171-172**: 124–136. doi:10.1016/j.agrformet.2012.11.008

Rosentreter, J. A., and others. 2021. Half of global methane emissions come from highly variable aquatic ecosystem sources. Nat. Geosci. **14**: 225–230. doi:10.1038/s41561-021-00715-2

Saunois, M., and others. 2020. The global methane budget 2000-2017. Earth System Science Data **12**: 1561–1623. doi:10.5194/essd-12-1561-2020

Sepúlveda-Jauregui, A., J. Hoyos-Santillán, F. J. Gutiérrez-Mendieta, R. Torres-Alvarado, L. Dendooven, and F. Thalasso. 2013. The impact of anthropogenic pollution on limnological characteristics of a subtropical highland reservoir "Lago de Guadalupe", Mexico. Knowl. Manag. Aquat. Ecosyst. **410**: 4. doi:10.1051/kmae/2013059

Silva, J. P., A. Lasso, H. J. Lubberding, M. R. Peña, and H. J. Gijzen. 2015. Biases in greenhouse gases static chambers measurements in stabilization ponds: Comparison of flux estimation using linear and non-linear models. Atmos. Environ. **109**: 130–138. doi:10.1016/j.atmosenv.2015.02.068

Thalasso, F., K. Walter Anthony, O. Irzak, E. Chaleff, L. Barker, P. Anthony, P. Hanke, and R. González-Valencia. 2020. Technical note: Mobile open dynamic chamber measurement of methane macroseeps in lakes. Hydrol. Earth Syst. Sci. **24**: 6047–6058. doi:10.5194/hess-24-6047-2020

Villa, J. A., Y. Ju, T. Yazbeck, S. Waldo, K. C. Wrighton, and G. Bohrer. 2021. Ebullition dominates methane fluxes from the water surface across different ecohydrological patches in a temperate freshwater marsh at the end of the growing season. Sci. Total Environ. **767**: 144498. doi:10.1016/j.scitotenv.2020.144498

Willmott, C. J., and K. Matsuura. 2006. On the use of dimensioned measures of error to evaluate the performance of spatial interpolators. Int. J. Geograph. Inf. Sci. **20**: 89–102. doi:10.1080/13658810500286976

Xiao, S., and others. 2016. Theoretical model for diffusive greenhouse gas fluxes estimation across water-air interfaces measured with the static floating chamber method. Atmos. Environ. **137**: 45–52. doi:10.1016/j.atmosenv.2016.04.036

Acknowledgments

We thank the "Consejo Nacional de Ciencia y Tecnología (Conacyt)" for the financial support received (Project A3-S-75824), as well as for the support to Víctor Germán Rodríguez-García (grant #738652) and to Leobardo Ottmar Palma Gallardo (grant #669264). Frédéric Thalasso received a partial financial support from the Cape Horn International Center project (ANID, CHIC-FB210018). The authors thank David Flores Rojas for his technical support.

Conflict of Interest

The authors declare that they have no conflict of interest.

Submitted 23 June 2023
Revised 25 September 2023
Accepted 11 October 2023

Associate editor: Isaac Santos